Uniaxial Strain on Graphene: Raman Spectroscopy Study and Band-Gap Opening

Zhen Hua Ni,[†] Ting Yu,[†,*] Yun Hao Lu,[‡] Ying Ying Wang,[†] Yuan Ping Feng,[‡] and Ze Xiang Shen[†,*]

[†]Division of Physics and Applied Physics, School of Physical and Mathematical Sciences, Nanyang Technological University, Singapore 637371, and [‡]Department of Physics, National University of Singapore, 2 Science Drive 3, Singapore 117542

ABSTRACT Graphene was deposited on a transparent and flexible substrate, and tensile strain up to ~0.8% was loaded by stretching the substrate in one direction. Raman spectra of strained graphene show significant red shifts of 2D and G band (−27.8 and −14.2 cm^{-1} per 1% strain, respectively) because of the elongation of the carbon−carbon bonds. This indicates that uniaxial strain has been successfully applied on graphene. We also proposed that, by applying uniaxial strain on graphene, tunable band gap at *K* point can be realized. First-principle calculations predicted a band-gap opening of ~300 meV for graphene under 1% uniaxial tensile strain. The strained graphene provides an alternative way to experimentally tune the band gap of graphene, which would be more efficient and more controllable than other methods that are used to open the band gap in graphene. Moreover, our results suggest that the flexible substrate is ready for such a strain process, and Raman spectroscopy can be used as an ultrasensitive method to determine the strain.

KEYWORDS: graphene · strain · Raman · band gap · flexible substrate

Graphene consists of one flat layer of carbon atoms arranged in a honeycomb lattice, and it has attracted intensive interest since experimentally discovered in 2004.[1] Due to its special properties, such as the charge carriers mimicking massless relativistic Dirac fermions, the anomalous quantum Hall effect, and the ballistic transport even at room temperature,[2] graphene provides a promising future for fundamental studies and practical applications.

In order to make graphene a real technology, a special issue must be solved: creating an energy gap at *K* and *K*′ points in the Brillouin zone. Different attempts have been made by researchers, such as patterning graphene into a nanoribbon,[3] forming graphene quantum dots,[2] making use of multilayer graphene sheets, and applying an external electrical field.[4] According to the carbon nanotubes (CNTs) study, the strain will dramatically change the electronic structure of CNTs.[5−7] It is shown that strain can open a band gap in a metallic CNT and modify the band gap in a semiconducting CNT with about 100 meV per 1% stretch.[7] Being a one-atom-thick structure, it is reasonable to predict that strain, especially uniaxial strain, can dramatically modify the electronic and optical properties of graphene. Moreover, since the two carbon sublattices of graphene are inequivalent under uniaxial strain, it is possible to introduce a band-gap opening on graphene due to the breaking of sublattice symmetry.[8−10] As an example, a band-gap opening is predicted for graphene growth on hexagonal boron nitride substrate due to the breaking of the equivalence of sublattice.[10]

In this study, we have successfully deposited the graphene sheets on a transparent flexible substrate: polyethylene terephthalate (PET). Uniaxial tunable tensile strain (up to ~0.8%) was applied on the single/three-layer graphene by stretching the PET in one direction, as justified later. Raman spectroscopy was used to study the strain effect on graphene. Significant red shift of the Raman 2D band (−27.8 cm^{-1} per 1% strain (/%)) and G band (−14.2 cm^{-1}/%) for single-layer graphene was observed under the uniaxial tensile strain. Our first-principle simulation of the band structure of single-layer graphene shows a band-gap opening of 300 meV for 1% strain, which provides an alternative way to fabricate graphene-based devices.

RESULTS AND DISCUSSION

Figure 1 shows the Raman spectra of single- and three-layer graphene on PET. Raman spectra of graphene on different substrates have been studied previously, and weak dependence of Raman bands on the substrates was observed.[11,12] In Figure 1, the Raman fingerprint of single-layered graphene, a very sharp (~30 cm^{-1}) and symmetric 2D band at around 2680 cm^{-1},

*Address correspondence to yuting@ntu.edu.sg, zexiang@ntu.edu.sg.

Received for review July 21, 2008 and accepted October 17, 2008.

Published online October 30, 2008.
10.1021/nn800459e CCC: $40.75

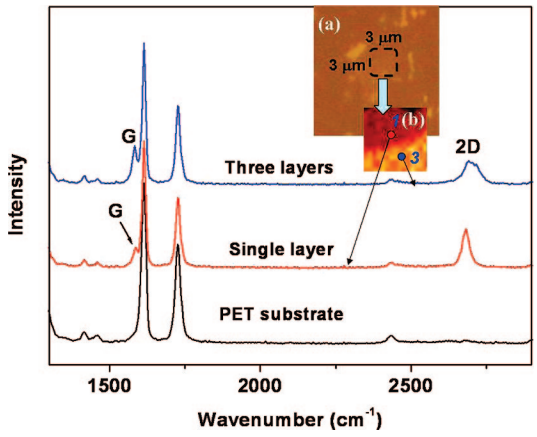

Figure 1. Raman spectra of single- and three-layer graphene as well as the spectrum of the PET substrate. Inset (a) is the optical image of the graphene on the PET substrate, with the chosen area for the Raman image study. Inset (b) is the 2D width Raman image of the chosen area. The dark region with a peak width of ~30 cm^{-1} corresponds to the single-layer graphene, while the bright region below corresponds to the three-layer graphene.

is clearly present.[13,14] In contrast, the 2D band of three-layer graphene is much broader (~59 cm^{-1}) and can be fitted by multipeaks. The change of 2D band with the increase of graphene thickness was explained by the evolution of electronic band structure of graphene[13] according to the double resonance theory. The Raman G band originates from the in-plane vibrational E_{2g} phonon and locates at ~1580 cm^{-1}. In our work, the G band of graphene overlaps with a strong peak from PET and appears as a weak shoulder. This makes it difficult to perform a detailed and careful study, such as a Raman image study. Instead, we used two Lorentzian curves to fit the spectra and obtained the frequency of G band at different points of the sample and then carried out the data analysis. The inset (a) in Figure 1 is the optical image of the graphene of interest. The optical contrast of graphene on PET is very poor compared to that of graphene on Si/SiO_2 substrate,[15] which makes the graphene barely visible by an optical microscope. The inset Raman image (b) in Figure 1 is constructed by the width of the Raman 2D band of the chosen area, which clearly shows the single- (dark region, with bandwidth about 30 cm^{-1}) and three-layer graphene (bright region, with bandwidth about 59 cm^{-1}). The following strain studies were carried out on the same graphene sheets.

Figure 2a presents the 2D frequency Raman images of unstrained (a1), strained (0.18% (a2), 0.35% (a3), 0.61% (a4), and 0.78% (a5) strain), and relaxed (a6) graphene by extracting the frequency of the 2D band. The Raman images were constructed by taking the peak frequencies of 2D bands of every point. The scales of all Raman images are from 2650 to 2710 cm^{-1}. In those images, the darker color represents lower 2D band frequency. Obviously, with the increase of strain (a2 to a5), the Raman images become darker and darker, indicating a universal red shift of the 2D band over the strained graphene. This red shift of the 2D band (and also the G band later) can be understood on the basis of the elongation of the carbon−carbon bonds, which weakens the bonds and therefore lowers their vibrational frequency. The spectra in the right-hand side of Figure 2a show the 2D band of SLG of unstrained (a1), 0.78% strained (a5), and relaxed graphene (a6). The red shift of the 2D band under strain as well as the blue shift due to strain relaxation is clearly seen.

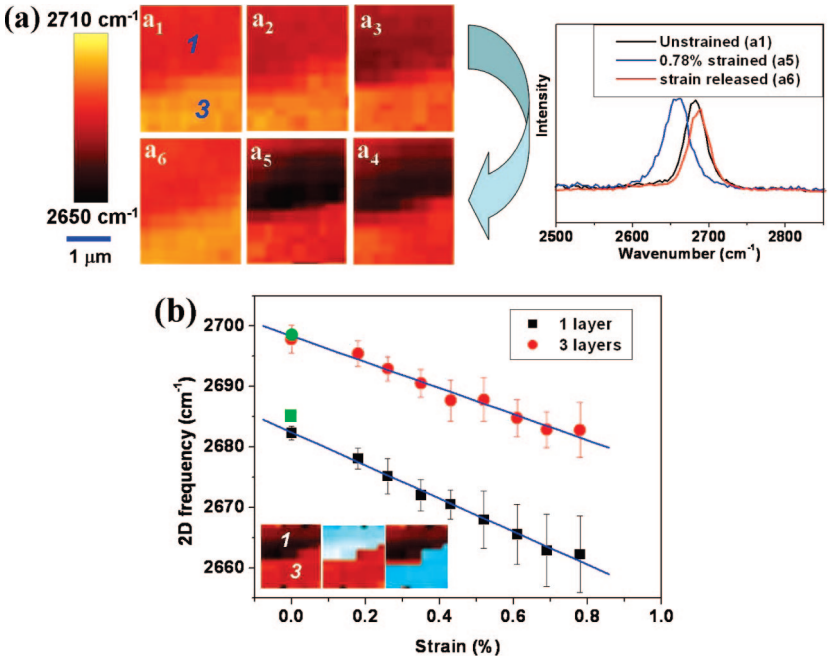

Figure 2. (a) Two-dimensional frequency Raman images of unstrained (a1), 0.18% (a2), 0.35% (a3), 0.61% (a4), and 0.78% (a5) strained, and relaxed (a6) graphene. The scale bar of all the images is 2650 to 2710 cm^{-1}. The Raman spectra on the right-hand side are taken from the 2D band SLG of a1, a5, and a6. (b) The analyzed 2D band frequency of single- (black squares) and three (red circles)-layer graphene under different uniaxial strain, from the highlighted area of inset figures. The green square/circle is the frequencies of relaxed graphene. The blue lines are the curve fit to the data. The slope is −27.8 cm^{-1}/% for single-layer graphene and −21.9 cm^{-1}/% for three-layer graphene.

To quantify the strain coefficient, Figure 2b shows the 2D band frequency from the same region of unstrained, strained, and relaxed graphene. The mean frequencies of the 2D band from the highlighted area, as shown in the inset of Figure 2b, were plotted as a function of strain with the standard deviation as errors. The absence of discrete jumps in the 2D band frequencies of graphene under different strain assures no slippage of graphene occurs during the stretching process. In Figure 2b, a linear dependence of the 2D band frequency on strain is clearly seen, with a slope of −27.8 ± 0.8 cm^{-1}/% for single-layer graphene and −21.9 ± 1.1 cm^{-1}/% for three-layer graphene. Both of these values are comparable to that of SWNTs (−7.9

$\sim -37.3\ cm^{-1}/\%$).[16−18] The high strain sensitivity of graphene successfully demonstrates its potential as an ultrasensitive strain senor as has been proved using the CNTs.[16] The linear dependence of Raman bands with strain is expected according to the phonon deformation potentials. The frequency shift of the Raman band is related to the uniaxial strain and the shear strain. The shear strain has a much smaller contribution,[19] which can be ignored for simplicity. The Raman frequency is then related to the strain by[19,20]

$$\frac{\Delta\omega}{\omega_0} = \gamma \cdot (\varepsilon_{xx} + \varepsilon_{yy})$$

where $\gamma = 1.24$ is the Güneisen parameter obtained from the experiment on CNTs;[19] ϵ_{xx} is the uniaxial strain, while $\epsilon_{yy} \approx -0.186\epsilon_{xx}$ is the relative strain in the perpendicular direction according to the Poisson's ratio of graphene;[21] ω_0 is the Raman band frequency. Therefore, as a rough estimation, the 2D band frequency ($\omega_0 \approx 2680\ cm^{-1}$) dependence on uniaxial tensile strain is

$$\frac{\Delta\omega}{\varepsilon} = -\omega_0 \cdot \gamma \cdot (1 - 0.186) = -27.1\ cm^{-1}/\%$$

This value is very close to our experimental result of single-layer graphene ($-27.8\ cm^{-1}/\%$). The 2D frequencies of graphene on PET are very uniform (with distribution of only $1\ cm^{-1}$) before the application of strain. However, the bigger error bars under higher strain indicate the wide distribution of 2D band frequency, reflecting the non-uniformity of local strain of single-layer graphene. Once the strain is released, the 2D band shifts upward and goes back immediately to almost the original position, indicating good strain reversibility of graphene. Such reversible and quick recovery property demonstrates the excellent elasticity of graphene, which might be critical for practical applications.

Because the G band is only a small shoulder peak, it is impossible for us to conduct the Raman imaging with the G band frequency. Raman spectra are taken from different positions (~10 positions) of the single- and three-layer graphene, and the spectra are curve fitted to obtain the G band frequency. The frequencies of the G band under different strain are shown in Figure 3, where the bigger error bar of the single-layer graphene is caused by the poor signal of the G band compared to the overlapping peak from the PET substrate, which would introduce a large fitting error. A linear dependence of the G band frequency on the strain is also clearly seen, with a slope of $-14.2 \pm 0.7\ cm^{-1}/\%$ for single-layer graphene and $-12.1 \pm 0.6\ cm^{-1}/\%$ for three-layer graphene. These values are also comparable to the results of CNTs, which is $11-17\ cm^{-1}/\%$.[16] The relative larger shifts of both G and 2D bands of single-layer graphene compared to those of three-layer

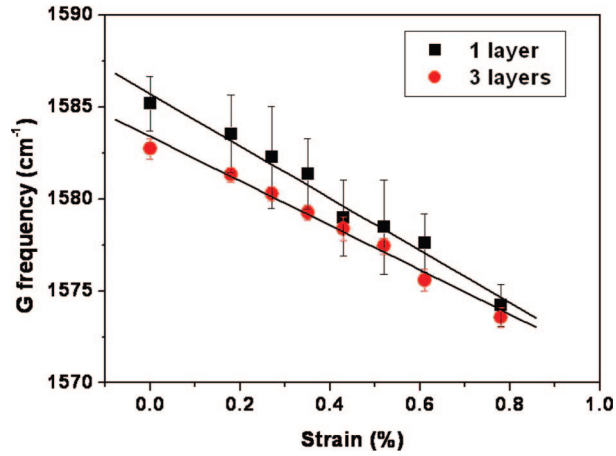

Figure 3. The G band frequency of single-layer (black squares) and three-layer (red circles) graphene under uniaxial strain. The black lines are the curve fit to the data. The slope is $-14.2\ cm^{-1}/\%$ for single-layer graphene and $-12.1\ cm^{-1}/\%$ for three-layer graphene.

graphene might be because strain is more effectively applied on thinner graphene sheet. The strain on graphene sheets was loaded by stretching the PET substrate, which interacts with graphene by van der Waals force. Therefore, it would be more difficult for strain to be transferred to thicker samples. One support for this interpretation is that no Raman band shift is observed on bulk graphite in the whole strain experiment, which means that the graphite is not affected by stretching the PET substrate.

Both the red shifts of 2D and G bands of graphene indicate that the graphene sheet experiences noticeable and controllable uniaxial strain by stretching the flexible substrate. The uniaxial strain in the current work is different from the biaxial strain we observed in epitaxial graphene[22] and graphene after deposition of a SiO_2 layer and annealing.[23] The uniaxial strain would affect the electronic properties of graphene much more significantly as it breaks the equivalence of sublattice of graphene.

To understand the strain dependence of the electronic structure of graphene, we carried out first-principle electronic band structure calculations of graphene under a uniaxial tensile strain. The schematic diagram of tensile strain application on the graphene lattice is shown in Figure 4a. A stretching in one direction results in a shrinking in another (perpendicular) direction. As an example, the band structures of unstrained and 1% strained graphene along the $I'-K-M$ are shown in Figure 4b,c, respectively. A band-gap opening of the strained graphene at the K point of the Brillouin zone is clearly seen. This band-gap opening can be attributed to the breaking of sublattice symmetry[8−10] of graphene under uniaxial strain. In general, the size of the band gap increases almost linearly with the increase of tensile strain, as shown in Figure 5, and for a strain of 1%, the band gap reaches about 300 meV. The density of states of the unstrained

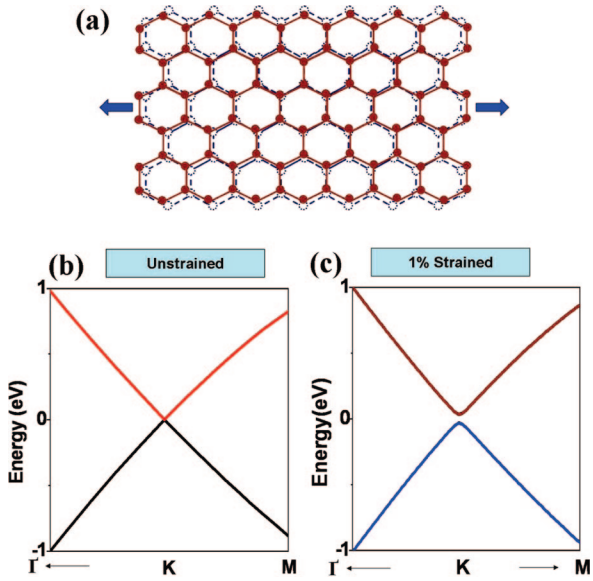

Figure 4. (a) Schematic representation of the effect of uniaxial tensile stress on a graphene supercell. The dashed (solid) lattices indicate the unstrained (strained) graphene. Calculated band structure of unstrained (b) and 1% tensile strained (c) graphene. A band gap is clearly seen on the band structure of strained graphene.

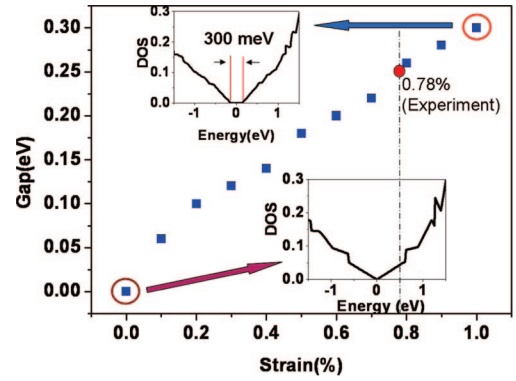

Figure 5. Band gap of strained graphene with the increase of uniaxial tensile strain on graphene. The magnitude of the gap is determined by the gap opening of the density of states. The insets show the calculated density of states (DOS) of unstrained and 1% tensile strained graphene. The dashed line and red solid dot indicate the calculated band gap of graphene under the highest strain (0.78%) in our experiment.

and 1% strained graphene are also shown in the insets of Figure 5, where the band gap in the strained graphene is clearly seen. The band gap corresponding to the highest strain obtained in our experiment (0.78%) is indicated by the red dot, and it is about 250 meV. The band-gap variation with uniaxial strain suggests that, by applying a uniaxial strain, a tunable band gap of single-layer graphene can be achieved. The band-gap opening by uniaxial strain would be more efficient compared to other methods, such as electric field tuning on bilayer[4] or molecule adsorption.[9] It is also easier to be realized than fabrication of graphene nanoribbons,[3] and the gap is more controllable than those in epitaxial graphene.[8] The uniaxial strained graphene provides an alternative way to fabricate graphene-based devices. In addition to the flexible substrate, graphene can also be deposited on piezocrystal so that the strain can be easily and precisely controlled. Further experiments will be carried out to study the transport properties of uniaxial strained graphene and correlate with the simulated band structure.

CONCLUSION

In summary, we have deposited single- and three-layer graphene on a transparent and flexible substrate, PET. By stretching the PET, uniaxial strain of ~0.8% can be applied on graphene. Raman spectroscopy studies of strained graphene show significant red shift of G and 2D band (−14.2 and −27.8 cm^{-1}/%, respectively for single-layer graphene). Finally, results of our first-principle calculations suggest that a band-gap opening of ~300 meV can be achieved by applying 1% uniaxial strain on graphene. The strained graphene provides an alternative way to experimentally tune the band gap of single-layer graphene, which is more efficient and more controllable than the other techniques that are used to open a band gap in graphene.

EXPERIMENTAL AND COMPUTATIONAL SECTION

The graphene sample was prepared by mechanical cleavage[1,15] from a highly ordered pyrolytic graphite (HOPG, Structure Probe, Inc./SPI Supplies) and transferred onto a PET film. Tensile strain on graphene sheets was loaded by stretching the PET film in one direction. The amount of strain is determined by dividing the extra length with the unstrained length. Because the graphene is ultrathin, the van der Waals force between substrate and graphene would be strong enough to exert the strain (~1%) on graphene.[24] The Raman spectra were carried out with a WITEC CRM200 Raman system. The excitation source is a 532 nm laser (2.33 eV) with a laser power below 0.1 mW on the sample to avoid laser-induced local heating.[25] A 100× objective lens with a numerical aperture (NA) of 0.95 was used in the Raman experiments, and the spot size of a 532 nm laser was estimated to be 500 nm. For the Raman image, the sample was placed on an $x-y$ piezostage and scanned under the illumination of a laser. The Raman spectra from every spot of the sample were recorded. The stage movement and data acquisition were controlled using ScanCtrl Spectroscopy Plus software from WITec GmbH, Germany. Data analysis was done by using WITec Project software. After the application of strain, the sample was located again and Raman imaging was carried out on the same area of the sample. First-principle calculations were performed using the VASP code.[26,27] The projector augmented wave potentials were used for electron−ion interactions, while the local spin density approximation (LSDA) was used for exchange−correlation function. For the Brillouin zone integrations, we used a 45 × 45 × 1 grid of Monkhorst−Pack special points together with a Gaussian smearing of 0.1 eV for the one-electron eigenvalues. The plane wave basis set was restricted by a cutoff energy of 400 eV. The lattice constant of unstrained graphene structure was set to 0.242 nm, which is the lattice parameter determined from our first-principle calculations within LSDA. The strained graphene was obtained by applying extension on x-axes (y-axes) with a fixed value, while the value of y-axes (x-axes) was tuned as the system reaches its lowest total

energy. In structure relaxation, atoms were fully relaxed until the interatomic forces were less than 0.1 eV/nm.

REFERENCES AND NOTES

1. Novoselov, K. S.; Geim, A. K.; Morozov, S. V.; Jiang, D.; Zhang, Y.; Dubonos, S. V.; Grigorieva, I. V.; Firsov, A. A. Electric Field Effect in Atomically Thin Carbon Films. *Science* **2004**, *306*, 666–669.
2. Geim, A. K.; Novoselov, K. S. The Rise of Graphene. *Nat. Mater.* **2007**, *6*, 183–191.
3. Han, M. Y.; Ozyilmaz, B.; Zhang, Y. B.; Kim, P. Energy Band-Gap Engineering of Graphene Nanoribbons. *Phys. Rev. Lett.* **2007**, *98*, 206805/1–206805/4.
4. Castro, E. V.; Novoselov, K. S.; Morozov, S. V.; Peres, N. M. R.; Dos Santos, J.; Nilsson, J.; Guinea, F.; Geim, A. K.; Neto, A. H. C. Biased Bilayer Graphene: Semiconductor with a Gap Tunable by the Electric Field Effect. *Phys. Rev. Lett.* **2007**, *99*, 216802/1–216802/4.
5. Yang, L.; Han, J. Electronic Structure of Deformed Carbon Nanotubes. *Phys. Rev. Lett.* **2000**, *85*, 154–157.
6. Heyd, R.; Charlier, A.; McRae, E. Uniaxial-Stress Effects on the Electronic Properties of Carbon Nanotubes. *Phys. Rev. B* **1997**, *55*, 6820–6824.
7. Minot, E. D.; Yaish, Y.; Sazonova, V.; Park, J.-Y.; Brink, M.; McEuen, P. L. Tuning Carbon Nanotube Band Gaps with Strain. *Phys. Rev. Lett.* **2003**, *90*, 156401/1–156401/4.
8. Zhou, S. Y.; Gweon, G. H.; Fedorov, A. V.; First, P. N.; De Heer, W. A.; Lee, D. H.; Guinea, F.; Neto, A. H. C.; Lanzara, A. Substrate-Induced Bandgap Opening in Epitaxial Graphene. *Nat. Mater.* **2007**, *6*, 770–775.
9. Ribeiro, R. M.; Peres, N. M. R.; Coutinho, J.; Briddon, P. R. Inducing Energy Gaps in Monolayer and Bilayer Graphene: Local Density Approximation Calculations. *Phys. Rev. B* **2008**, *78*, 075442/1–075442/7.
10. Giovannetti, G.; Khomyakov, P. A.; Brocks, G.; Kelly, P. J.; van den Brink, J. Substrate-Induced Band Gap in Graphene on Hexagonal Boron Nitride: *Ab Initio* Density Functional Calculations. *Phys. Rev. B* **2007**, *76*, 073103/1–073103/4.
11. Wang, Y. Y.; Ni, Z. H.; Yu, T.; Wang, H. M.; Wu, Y. H.; Chen, W.; Wee, A. T. S.; Shen, Z. X. Raman Studies of Monolayer Graphene: The Substrate Effect. *J. Phys. Chem. C* **2008**, *112*, 10637–10640.
12. Calizo, I.; Bao, W. Z.; Miao, F.; Lau, C. N.; Balandin, A. A. The Effect of Substrates on the Raman Spectrum of Graphene: Graphene-on-Sapphire and Graphene-on-Glass. *Appl. Phys. Lett.* **2007**, *91*, 201904/1–201904/3.
13. Ferrari, A. C.; Meyer, J. C.; Scardaci, V.; Casiraghi, C.; Lazzeri, M.; Mauri, F.; Piscanec, S.; Jiang, D.; Novoselov, K. S.; Roth, S.; et al. Raman Spectrum of Graphene and Graphene Layers. *Phys. Rev. Lett.* **2006**, *97*, 187401/1–187401/4.
14. Graf, D.; Molitor, F.; Ensslin, K.; Stampfer, C.; Jungen, A.; Hierold, C.; Wirtz, L. Spatially Resolved Raman Spectroscopy of Single- and Few-Layer Graphene. *Nano Lett.* **2007**, *7*, 238–242.
15. Ni, Z. H.; Wang, H. M.; Kasim, J.; Fan, H. M.; Yu, T.; Wu, Y. H.; Feng, Y. P.; Shen, Z. X. Graphene Thickness Determination Using Reflection and Contrast Spectroscopy. *Nano Lett.* **2007**, *7*, 2758–2763.
16. Cronin, S. B.; Swan, A. K.; Unlu, M. S.; Goldberg, B. B.; Dresselhaus, M. S.; Tinkham, M. Resonant Raman Spectroscopy of Individual Metallic and Semiconducting Single-Wall Carbon Nanotubes under Uniaxial Strain. *Phys. Rev. B* **2005**, *72*, 035425/1–035425/8.
17. Cooper, C. A.; Young, R. J. Investigation of Structure/Property Relationships in Particulate Composites through the Use of Raman Spectroscopy. *J. Raman Spectrosc.* **1999**, *30*, 929–938.
18. Cronin, S. B.; Swan, A. K.; Unlu, M. S.; Goldberg, B. B.; Dresselhaus, M. S.; Tinkham, M. Measuring the Uniaxial Strain of Individual Single-Wall Carbon Nanotubes: Resonance Raman Spectra of Atomic-Force-Microscope Modified Single-Wall Nanotubes. *Phys. Rev. Lett.* **2004**, *93*, 167401/1–167401/4.
19. Reich, S.; Jantoljak, H.; Thomsen, C. Shear Strain in Carbon Nanotubes under Hydrostatic Pressure. *Phys. Rev. B* **2000**, *61*, R13389–R13392.
20. Thomsen, C.; Reich, S.; Ordejon, P. *Ab Initio* Determination of the Phonon Deformation Potentials of Graphene. *Phys. Rev. B* **2002**, *65*, 073403/1–073403/3.
21. Liu, F.; Ming, P. M.; Li, J. *Ab Initio* Calculation of Ideal Strength and Phonon Instability of Graphene under Tension. *Phys. Rev. B* **2007**, *76*, 064120/1–064120/7.
22. Ni, Z. H.; Chen, W.; Fan, X. F.; Kuo, J. L.; Yu, T.; Wee, A. T. S.; Shen, Z. X. Raman Spectroscopy of Epitaxial Graphene on a SiC Substrate. *Phys. Rev. B* **2008**, *77*, 115416/1–115416/6.
23. Ni, Z. H.; Wang, H. M.; Ma, Y.; Kasim, J.; Wu, Y. H.; Shen, Z. X. Tunable Stress and Controlled Thickness Modification in Graphene by Annealing. *ACS Nano* **2008**, *2*, 1033–1039.
24. Son, H.; Samsonidze, G. G.; Kong, J.; Zhang, Y. Y.; Duan, X. J.; Zhang, J.; Liu, Z. F.; Dresselhaus, M. S. Strain and Friction Induced by van der Waals Interaction in Individual Single Walled Carbon Nanotubes. *Appl. Phys. Lett.* **2007**, *90*, 253113/1–253113/3.
25. Calizo, I.; Balandin, A. A.; Bao, W.; Miao, F.; Lau, C. N. Temperature Dependence of the Raman Spectra of Graphene and Graphene Multilayers. *Nano Lett.* **2007**, *7*, 2645–2649.
26. Kresse, G.; Hafner, J. *Ab Initio* Molecular Dynamics for Liquid Metals. *Phys. Rev. B* **1993**, *47*, 558–561.
27. Kresse, G.; Furthmuller, J. Efficient Iterative Schemes for *Ab Initio* Total-Energy Calculations Using a Plane-Wave Basis Set. *Phys. Rev. B* **1996**, *54*, 11169–11186.